Imaging of Lymph Node Uptake After Intravenous Administration of Indium-111 Metalloporphyrins

G.D. Robinson, Jr., Abass Alavi, Richard Vaum, and Muni Staum

Nuclear Medicine Section, Department of Radiology and Cerebrovascular Research Center, Department of Neurology, University of Pennsylvania School of Medicine, Philadelphia, Pennsylvania

Indium-111- (^{111}In) labeled tetra (*N,N,N*-trimethylanilinium) porphyrin (TTAP), tetra (*N*-methyl-4-pyridyl)porphyrin (TMPyP), and tetra(4-sulfonatophenyl)porphyrin (T4SPP) were snythesized and lymph node uptake was measured in animals after intravenous administration. In rats [^{111}In] TTAP had maximum lymph node to muscle uptake ratios which averaged 85:1 between 24 and 48 hr postinjection. Total lymph node uptake was nearly 1% at that time. Lymph nodes in rabbits were clearly visualized by gamma scintigraphy at 48 hr after i.v. injection of labeled TTAP. These results suggest that ^{111}In-labeled TTAP may be a prototype for the development of a class radiopharmaceuticals which permits visualization of lymph nodes after i.v. administration.

J Nucl Med 27:239–242, 1986

The evaulation of the lymphatic system by radionuclide imaging has become important in the diagnosis of primary lymph node disorders, as well as in serving as a major indicator of the presence of metastasis, and its extent, in nonlymphatic malignant diseases. Currently employed techniques such as oil lymphangiography and technetium-99m (^{99m}Tc) antimony sulfide lymphoscintigraphy, have significant limitations (*1–3*). Intravenous lymphoscintigraphy offers the potential of noninvasive evaluation of mediastinal, mesenteric, cervical, and other deep-seated, less accessible nodes, such as the para-aortic and inguinal, which cannot be studied by more conventional techniques.

In the 1940s, porphyrins and metalloporphyrins were administered intravenously and used to improve visual detection of neoplastic tissue for surgical removal (*4–5*). Since that time, i.v. administered radioactive metalloporphyrins have been studied for a variety of purposes, especially for lymphatic ablation (*6–9*), but no diagnostic applications have been reported.

To test the potential usefulness of labeled, water soluble porphyrin derivatives as radiodiagnostic agents for lymph node imaging after i.v. administration, tetra(*N*-methyl-4-pyridyl)porphyrin tetratosylate (TMPyP), tetra(*N,N,N*-trimethylanilinium) porphyrin tetrachloride (TTAP), and tetrasodium tetra(4-sulfonatophyenyl) porphyrin dodecahydrate (T4SPP) were labeled with ^{111}In and administered i.v. to rats for direct tissue assay and to rabbits for scintillation camera imaging. TTAP and T4SPP were chosen for comparison with TMPyP (*10*), because they represent two kinds of modification of the porphyrin structure (strong cation and strong anion) which might be expected to produce a change in biodistribution. The structures for the unlabeled porphyrin derivatives are shown in Fig. 1*.

MATERIALS AND METHODS

For the biodistribution studies in animals, the desired amount of no-carrier-added [^{111}In]chloride solution was diluted to a total volume of 2.0 ml with 0.2*M* acetate buffer (pH = 4.5), and 2.0×10^{-3} mmole of porphyrin derivative were added. The final pH of this reaction mixture was 4.3 to 4.5. Labeling proceeded to more than 97% completion by autoclaving the mixture for 30 in 121°C. Radiochemical yield was verified by taking a 50-μl aliquot of the product solution and

Received May 13, 1985; revision accepted Oct. 8, 1985.

For reprints contact: Abass Alavi, MD, Nuclear Medicine Section, Hospital of the University of Pennsylvania, 3400 Spruce St./Gl, Philadelphia, PA 19104.

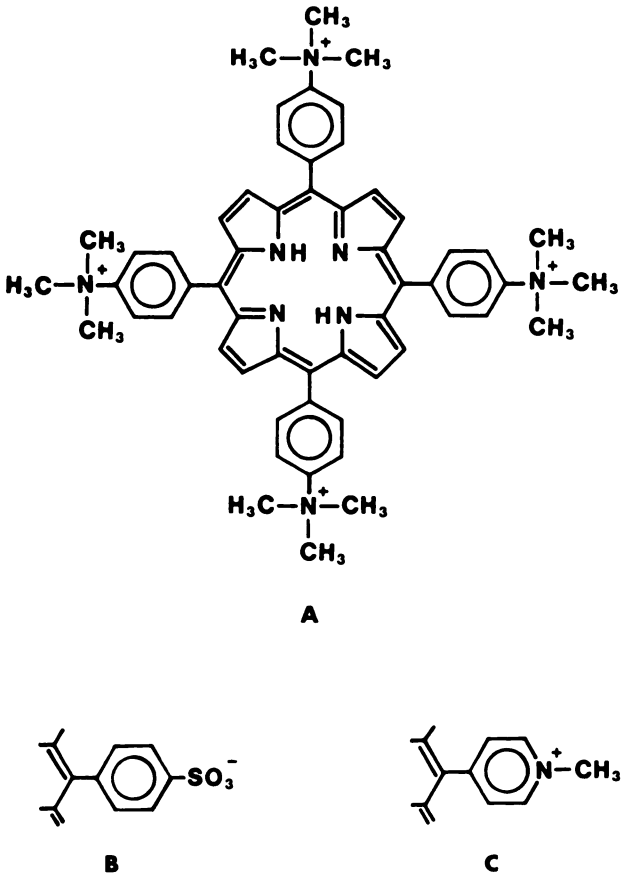

FIGURE 1
Structures of water soluble porphyrin derivatives used in these studies: A: Tetra(*N,N,N*-Trimethylanilinium)porphyrin (TTAP); B: Tetra(4-Sulfonatophenyl)porphyrin(T4SPP); and C: Tetra(*N*-Methyl-4-pyridyl)porphyrin (TMPyP)

extracting the unbound ^{111}In from 0.2*M* acetate buffer (pH = 4.5) into 0.1*M* 8-hydroxyquinoiline in $CHCl_3$. The labeled porphyrin derivatives were used without further purification.

Preliminary biodistribution studies by direct tissue assay were performed using 250 g, male Wistar rats. Three groups of 12 rats were anesthetized by ether inhalation and the animals in each group received ~100 μCi each of one of the three labeled porphyrin derivatives in 200 μl of aqueous acetate-buffered solution through tail vein injection. For each derivative, three rats were killed at 1, 4, 24, and 48 hr. Dissection included: cervical, thoracic, axillary, abdominal, GI, and popliteal lymph nodes. A reference blood sample was obtained by cardiac puncture while the animals were under anesthesia immediately prior to killing.

Scintillation camera imaging studies were performed using six 2.3-kg white rabbits. For each [^{111}In]porphyrin derivative, 200 μl of aqueous solution containing 200 μl of labeled porphyrin were injected into an ear vein of two rabbits. The distribution of ^{111}In in each of the six rabbits was then imaged from the anterior projection at 4, 8, 24, 72, and 96 hr postinjection. At each imaging interval the rabbits were sufficiently sedated to obtain one anterior view containing 300k counts with the scintillation camera analyzer set to include both the 173 keV and 246 keV photons of ^{111}In.

RESULTS

Results of biodistribution studies in rats (Table 1) indicate that the patterns of ^{111}In uptake and turnover are similar for all three labeled porphyrin derivatives. Substantial accumulation of ^{111}In in liver and kidneys is evident in each case. Blood clearance was notably slower with the labeled T4SPP derivative than for either TMPyP or TTAP (Table 2). Indium-111 TTAP showed the highest lymph node-to-muscle uptake ratios, which averaged 85:1 during the time interval between 24 and 48 hr postinjection. These results are illustrated in Fig. 2. Uptake in the nodal groups which were excised was observed for all time intervals studied (Table 1). At 48 hr postinjection total [^{111}In]TTAP nodal uptake was nearly 1% (0.761 ± 0.112%) of the injected dose (Table 1).

In the imaging studies, [^{111}In]TTA appeared to be superior to both TMPyP and T4SPP as indicated by delineation of the popliteal nodes. This nodal group was seen most clearly on the images obtained at 48 hr postinjection. These images are shown in Fig. 3. Nodes were seen at 4 hr postinjection with the labeled TTAP derivative, with gradually improving contrast up to 48 hr, and little further change noted on subsequent images. With [^{111}In]TMPyP, the popliteal nodes were

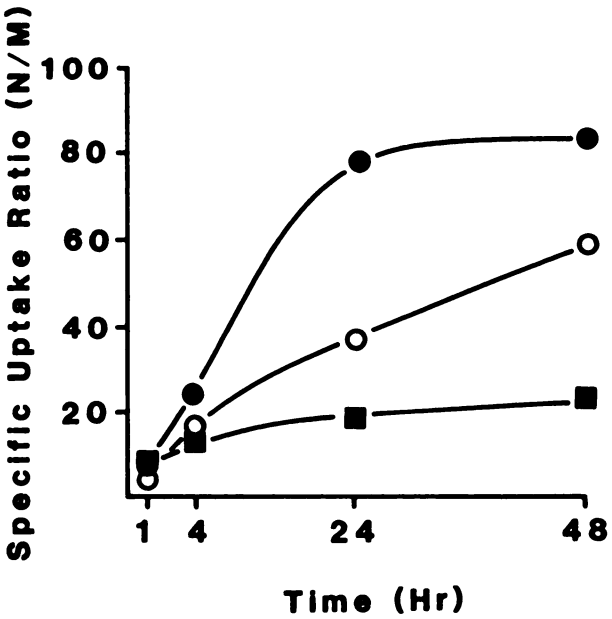

FIGURE 2
Specific uptake ratios for ^{111}In in lymph nodes of rat following i.v. injection of labeled metalloporphyrin. N = average nodal uptake (% dose/g); M = average muscle uptake (% dose/g); (●)TTAP, (O)TMPyP, (■)T4SPP

TABLE 1
Biodistributions of ^{111}In Following i.v. Administration of Labeled Metalloporphyrins in Male Rats*

Porphyrin	Time (hr)	Organ					
		Lymph nodes	Muscle	Liver	Kidney	GI Tract	Testes
TTAP	1	0.391 ± 0.063	18.6 ± 2.6	14.5 ± 1.3	5.57 ± 0.72	12.4 ± 0.9	0.571 ± 0.117
	4	0.509 ± 0.106	11.9 ± 1.4	22.5 ± 1.5	8.08 ± 0.65	9.54 ± 1.24	0.667 ± 0.071
	24	0.634 ± 0.093	8.04 ± 0.88	54.5 ± 16.0	16.6 ± 5.9	11.0 ± 0.1	0.395 ± 0.039
	48	0.761 ± 0.112	6.31 ± 0.73	41.7 ± 3.5	14.3 ± 2.4	6.93 ± 1.50	0.353 ± 0.025
TMPyP	1	0.343 ± 0.073	11.7 ± 1.6	3.94 ± 0.36	4.89 ± 0.90	4.88 ± 1.19	0.221 ± 0.024
	4	0.341 ± 0.111	7.53 ± 0.98	9.04 ± 1.16	10.3 ± 2.4	4.26 ± 1.17	0.444 ± 0.410
	24	0.292 ± 0.084	4.99 ± 0.63	12.0 ± 2.2	12.6 ± 1.3	3.34 ± 0.69	0.183 ± 0.031
	48	0.330 ± 0.069	4.88 ± 0.91	12.5 ± 2.3	14.4 ± 6.2	2.85 ± 1.04	0.200 ± 0.033
T4SPP	1	0.303 ± 0.068	7.31 ± 1.10	9.41 ± 2.86	2.83 ± 0.47	7.79 ± 1.55	0.774 ± 0.093
	4	0.270 ± 0.080	14.0 ± 2.7	15.6 ± 1.1	4.60 ± 0.22	6.15 ± 2.78	1.22 ± 0.12
	24	0.560 ± 0.123	13.0 ± 2.3	24.7 ± 4.3	7.49 ± 1.49	7.37 ± 0.96	0.912 ± 0.084
	48	0.442 ± 0.066	14.7 ± 1.8	29.4 ± 4.5	9.04 ± 0.60	6.08 ± 0.53	0.920 ± 0.056

* Mean %dose per organ (± s.d.) for three animals at each time interval.

faintly seen at 24 hr but no improvement in contrast was seen through 96 hr. Nodal visualization could not be demonstrated in the animals which received the labeled T4SPP derivative. In each case of nodal visualization, the popliteal nodes were most apparent, though uptake of activity in the cervical, abdominal, axillary, inguinal, and thoracic areas are consistent with uptake by lymph nodes which are known to lie in those regions.

DISCUSSION

The results of tissue assay of [^{111}In]porphyrin biodistribution suggest that, of the derivates studied, the labeled complexes of the positively charged porphyrins, TTAP and TMPyP, would be expected to be better candidates for use in lymph node imaging than would the negatively charged [^{111}In]T4SPP. Since lymph nodes generally overly muscle tissue, the ratio of uptake in lymph nodes to uptake in muscle was calculated as a predictor of the potential for imaging in vivo. Figure 2 demonstrates that lymph node-to-muscle (N/M) uptake ratios decreased in the order TTAP > TMPyP > T4SPP > during the time intervals studied. It was interesting to note that absolute nodal uptake (% dose) shows little increase beyond 4 hr postinjection. The increase in N/M which occurs for TTAP between 4 and 24 hr postinjection is a result of decreasing levels of ^{111}In in muscle tissue (Table 1). This is consistent with the finding that blood levels of [^{111}In]TTAP have decreased to 6.1% of the injected dose by 4 hr postinjection, and little increase in uptake in any organ would be likely after this time (Table 2).

It should be noted that, if blood activity is combined with the data presented in Table 1, then the total activity accounted for at 1 hr becomes 66 and 98% for TTAP and T4SPP, respectively. For the TMPyP derivative, only 35% of the administered dose is recovered. Renal excretion of the TMPyP derivative may be significant, and skeletal uptake appears to be substantial in the images obtained at 48 hr postinjection. Previously reported biodistribution data for the TMPyP derivative account for 36% of the dose at 1 hr (*10*). The other distribution results for the TMPyP derivative were comparable to those reported by Vaum et al. (*10*), except for blood levels which we found to be two to six times as high throughout the time intervals studied. These differences may be the result of differences in the preparative procedures used.

The scintillation camera imaging studies supported the results of the direct tissue ^{111}In assays. Although the general patterns of ^{111}In distribution were similar, with prominent renal and hepatic uptake noted for each derivative, specific individual differences were apparent. After administration of [^{111}In]T4SPP, blood-pool activity was prominent on the 4-hr image, but this was not noticeable at 24 hr postinjection. No regions of focal ^{111}In uptake which were consistent with nodal localization could be seen at any time of the intervals studied. Neither labeled TMPyP nor TTAP derivative

TABLE 2
Indium-111 Remaining in Blood*

Time (hr)	T4SPP	TMPyP	TTAP
1	3.50 ± 0.647	0.359 ± 0.120	0.714 ± 0.486
4	1.88 ± 0.687	0.279 ± 0.142	0.336 ± 0.216
24	0.618 ± 0.323	0.056 ± 0.021	0.022 ± 0.019
48	0.224 ± 0.167	0.030 ± 0.017	0.010 ± 0.012

* Mean %dose per organ (± s.d.) for three animals at each time interval.

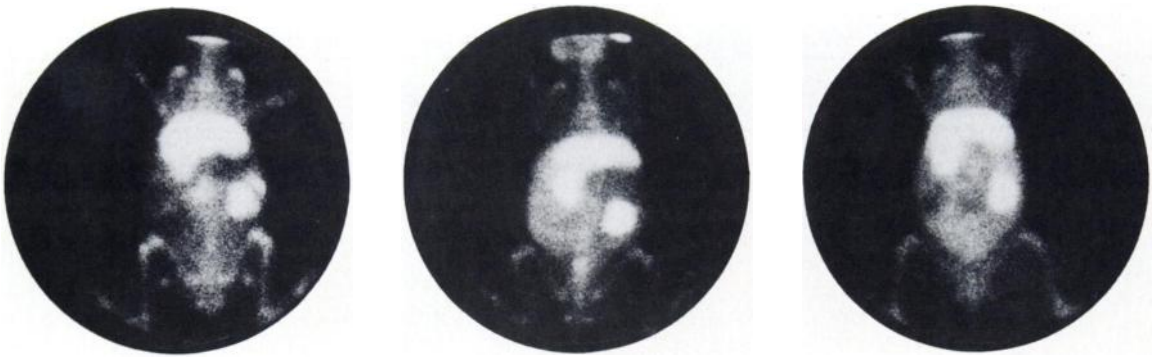

[^{111}In]TTAP [^{111}In]TMPYP [^{111}In]T4SPP

FIGURE 3
Anterior view scintillation camera images obtained 48 hr after i.v. injection of [^{111}In]porphyrin derivatives in rabbits. Note visualization of popliteal nodes with [^{111}]TTAP

showed prominent blood-pool activity at 4 hr postinjection, which is consistent with their more rapid clearances. With both of these derivatives, however, popliteal nodes were faintly visualized at 24 hr. By 48 hr these nodes were still faintly visualized in the animals which had received [^{111}In]TMPyP, but improved contrast resulted in clear visualization of popliteal nodes in the animals which received [^{111}In] TTAP (Fig. 3). In the latter animals, the popliteal nodes were seen on the latest images at 96 hr postinjection.

The mechanism of localization of these agents in lymph nodes is unclear. It has been suggested that porphyrins and metalloporphyrins are concentrated by tissues with a high mitotic index (*4*). Alternatively, they may localize in the region of the high endothelial venules which are unique to lymph nodes, as proposed for particulate antigens by Blau (*11*). Other possible mechanisms include extravasation from the systemic vessels and uptake by way of lymphatic tissue drainage pathways, or uptake through functional lymph node-venous communications as proposed by Anderson and Anderson (*12*). The poor uptake noted for [^{111}In]T4SPP may be related to its high amount of protein binding (*9*) and this may have some implications with regard to the mechanism of uptake. A better understanding of the mechanism by which this class by labeled compounds is taken up by lymph nodes is crucial if compounds with improved biologic behavior are to be developed on a rational basis. However, since the other imaging modalities which are used for lymphatic visualization suffer from serious shortcomings, the apparent potential usefulness of this class of compounds may represent an important advance in the detection and evaluation of the lymphatic system.

FOOTNOTES

* The porphyrin derivatives were purchased from Midcentury Chemicals, Posen, IL. They were used without further purification.

†Indium-111 choloride in acidic aqueous solution was purchased from Medi-Physics, Inc., Emeryville, CA.

REFERENCES

1. Kaplan WD, Whitemore WF, Gittes RF: Visualization of canine and human prostatic lymph nodes following intraprostatic injection of technetium-99m-antimony sulfide colloid. *Invest Radiol* 15:34–38, 1980
2. Ege GN: Internal mammary lymphoscintigraphy. The rationale, technique, interpretation and clinical application: A review based on 848 cases. *Radiology* 118:101–108, 1976
3. Kazem I, Nedwich A, Mortel R: Comparative histological changes in the normal lymph node following ethiodol lymphography and colloidal gold-198 lymphoscanning. *Clin Radiol* 22:382–388, 1971
4. Figge FHJ, Weiland GS, Manganiello LOJ: Cancer detection and therapy. Affinity of neoplastic, embryonic and traumatized tissues for porphyrins and metalloporphyrins. *Proc Soc Exp Biol Med* 68:640–641, 1948
5. Rasmussen-Taxdal DS, Ward GE II, Figge FHJ: Fluorescence of human lymphatic and cancer tissues following high doses of intravenous hematoporphyrin. *Cancer* 8:78–81, 1955
6. Nunn AD: The kinetics of incorporation of In-111 into m-Tetraphenylporphine. *J Radioanal Chem* 53:291–298, 1979
7. Fawwaz RA, Winchell HS, Frye F: Localization of ^{58}Co and ^{65}Pd-hematoporphyrin complexes in canine lymph nodes. *J Nucl Med* 10:581–585, 1969
8. Fawwaz RA, Hemphill W, Winchell HS: Potential use of ^{109}Pd-porphyrin complexes for selective lymphatic ablation. *J Nucl Med* 12:231–236, 1971
9. Fawwaz, RA, Frye, Laughman WD: Survival of skin homografts in dogs injected with Pd-protoporphyrin. *J Nucl Med* 15:997–1007, 1974
10. Vaum R, Heindel ND, Burns HD, et al: Synthesis and evaluation of an ^{111}In-labeled porphyrin for lymph node imaging. *J Pharm Sci* 71:1223–1226, 1982
11. Blau JN: Penetration of colloidal carbon through postcapillary venules in lymph nodes in Peyer's patches of the guinea-pig: A potential immunogenic route. *Br J Exp Pathol* 59:558–563, 1978
12. Anderson AO, Anderson ND: Studies on the structure and permeability of the microvasculature in normal rat lymph nodes. *Am J Pathol* 80:387–418, 1975